Modelling of 'no-tension' interfaces

Morten Andersen Herfelt[a)], Jørgen Krabbenhøft[a)], Kristian Krabbenhøft[b,1)]

[a)] *Optum Computational Engineering, Copenhagen, Denmark*
[b)] *Division of Civil Engineering, University of Liverpool, UK*

Abstract

The differences between two common approaches to the modelling of interfaces are discussed. Though very similar, the two different approaches lead to rather different results, qualitatively as well as quantitatively, when applied to typical boundary value problems. This is demonstrated with respect to the undrained bearing capacity of a strip footing subjected to general loading. Finally, the results of the two approaches are compared to common analytical bearing capacity expressions where similar differences are observed.

Key words: Undrained shear strength, interfaces, no-tension

1 Introduction

Undrained total stress modelling make use of cohesive failure criteria such as that of Tresca to account for undrained shear strength. Such failure criteria allow for tensile total stresses which may be justified by the possibility of tensile pore pressures that would render the effective stresses compressive. However, at interfaces between the soil and a structure (e.g. a foundation or a wall), a 'no-tension' condition is usually imposed to account for the fact that gaps or cracks may exit or form as a result of deformation, thus preventing tensile excess pore pressures from being generated.

Though the basic premise that tension should not be allowed at interface is well recognized, there appears to be no common agreement regarding the exact way in which the no-tension condition should be imposed. While details regarding the exact way in which interfaces are modelled often are not described in much detail, there appears to be two different approaches. Though superficially similar, these may nevertheless result in rather different overall behaviour of the system under consideration.

[1] Corresponding author. Email: kristian.krabbenhoft@liverpool.ac.uk

10 November 2020

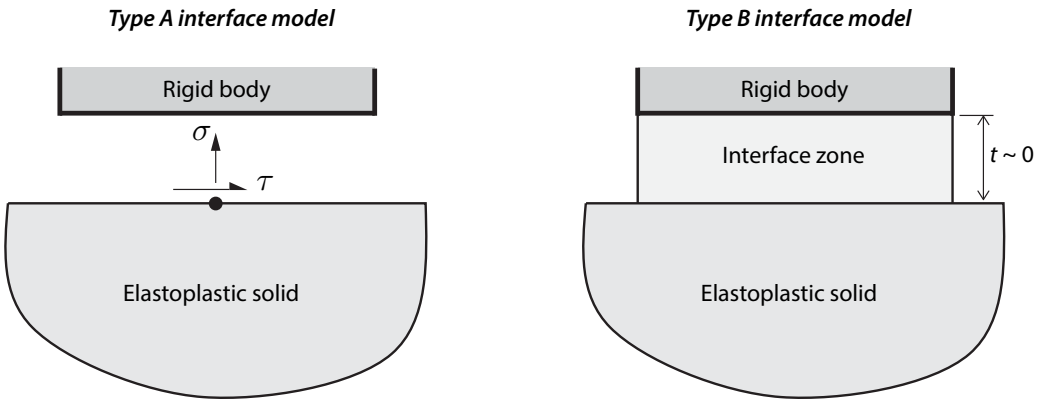

Fig. 1. Interface models of Types A and B.

In this note, the two different approaches to the modelling of interfaces are described after which their effects in terms predicting the bearing capacity of a strip footing subjected to general loading is discussed. Throughout the note, compressive stresses are positive and the principal stresses are ordered as $\sigma_1 \geq \sigma_2 \geq \sigma_3$.

2 Interface modelling

The two different approaches to imposing no-tension conditions are in many ways related to two different ways of modelling interfaces, either analytically or, more commonly, numerically using finite elements or similar. These are illustrated in Figure 1. In the first approach, in the following referred to as Type A, the no-tension condition is imposed with respect to the tractions on the surface of the elastoplastic solid in contact with the structure or foundation. In the context of finite elements, one would usually impose the no-tension condition with respect to the nodal forces on the relevant boundary following well-known procedures of computational contact mechanics (see e.g. Wriggers, 2006). In the second approach, in the following referred to as Type B, one imagines an infinitely thin layer of material between the elastoplastic solid and the rigid body. This interface zone has the same properties as the elastoplastic solid expect that no tension is allowed. In a finite element context, this approach corresponds to the use of interface elements which may be thought of as regular finite elements that have been collapsed, sometimes to attain a thickness identically equal to zero, but more often to a finite thickness sufficiently small to achieve the same physical response as a zero-thickness element without incurring the numerical difficulties such an element entails.

Next, interface conditions are imposed. For the Type A model, one impose limits on the

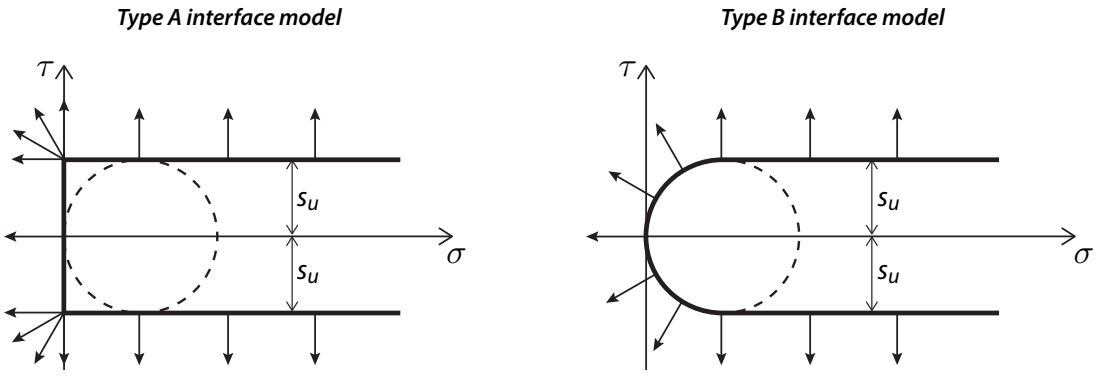

Fig. 2. Failure envelopes for interface models of Types A and B ($\alpha = 1$) with plastic strain rate vectors following the associated flow rule.

shear strength in combination with a no-tension condition:

$$\begin{aligned} |\tau| &\leq \alpha s_u \\ \sigma &\geq 0 \end{aligned} \tag{1}$$

where $\alpha \leq 1$ is a parameter that caters for a possible reduction of the shear strength at the interface relative to the shear strength of the soil. For the Type B model, the interface conditions are imposed in the same manner as the failure condition for the soil, e.g. in terms of principal stresses:

$$\begin{aligned} \sigma_1 - \sigma_3 &\leq 2\alpha s_u \\ \sigma_3 &\geq 0 \end{aligned} \tag{2}$$

The two conditions are shown in terms of σ versus τ in Figure 2. The dashed lines indicate the largest Mohr's circle contained within admissible strength domain. While superficially similar, the two interface models are manifestly different in terms of the combination of normal and shear stresses they allow for. Indeed, the status of the Type A model as a true 'no-tension' interface is questionable as it allows for stress states that in fact imply tension within the interface albeit the normal stress at the interface boundary is compressive at all times. The stress state $(\sigma, \tau) = (0, s_u)$, for example, corresponds to equal and opposite principal stresses equal to s_u and thus tension at an angle of 45° relative to the interface plane. Moreover, as pointed out by Houlsby & Puzrin (1999), the Type A model suffers from two other shortcomings: (i) shear stresses can be sustained immediately after separation and (ii) separation is never accompanied by tangential movement. The Type B model remedies these shortcomings to some extent in that pure separation is only possible for zero normal and shear stresses. However, tangential movement below $\sigma/|\tau| = 1$ is only possible for finite normal stresses. This feature is similar to that of the kind dilative response implied by a standard frictional interface assuming associated flow. The only way to remedy this feature is to adopt a nonassociated flow rule at the interface. To do this, first note that the no-tension condition $\sigma_3 \geq 0$ in fact is a special case of a

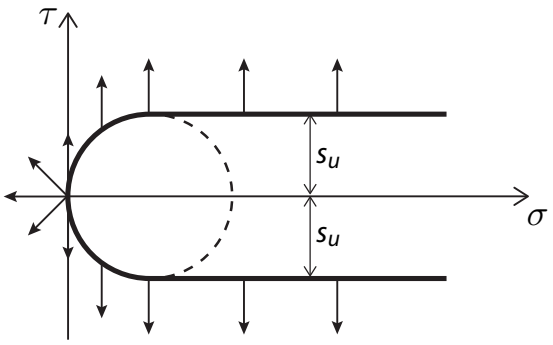

Fig. 3. Nonassociated version of Type B interface.

Mohr-Coulomb constraint given by

$$F = (\sigma_1 - \sigma_3) - (\sigma_1 + \sigma_3)\sin\phi_t \leq 0 \tag{3}$$

with $\phi_t = 90°$. This form suggests a flow potential given by

$$G = (\sigma_1 - \sigma_3) - (\sigma_1 + \sigma_3)\sin\psi \tag{4}$$

where $\psi = 0$ produces the kinematics indicated in Figure 3, i.e. an indeterminate combination of sliding and separation at $(\sigma, \tau) = (0, 0)$ and pure sliding for all other stress states. The adoption of such a flow rule introduces a number of well-known complications. Hence, for the remainder of this note the focus will be on the effects of the Type A and B models assuming associated flow for both.

2.1 Generalization of Type B interface

Suppose that the strength of the soil follows the Mohr-Coulomb criterion:

$$(\sigma_1 - \sigma_3) - (\sigma_1 + \sigma_3)\sin\phi - 2c\cos\phi \leq 0 \tag{5}$$

where c and ϕ are the cohesion and friction angle respectively. At interfaces, the same model may be assumed valid though with reduced material strengths:

$$(\sigma_1 - \sigma_3) - (\sigma_1 + \sigma_3)\sin\phi_i - 2c_i\cos\phi_i \leq 0 \tag{6}$$

where $c_i \leq c$ and $\phi_i \leq \phi$ are the interface cohesion and friction angle respectively. This criterion may be supplemented with a generalized tension cut-off given by

$$(\sigma_1 - \sigma_3) - (\sigma_1 + \sigma_3)\sin\phi_t - 2\sigma_t\sin\phi_t \leq 0 \tag{7}$$

where σ_t is the tensile strength and ϕ_t is a friction angle characterizing the slope of the cut-off. We note that the standard no-tension condition is recovered for $\sigma_t = 0$ and $\phi_t = 90°$. The combined failure surface is shown in Figure 4.

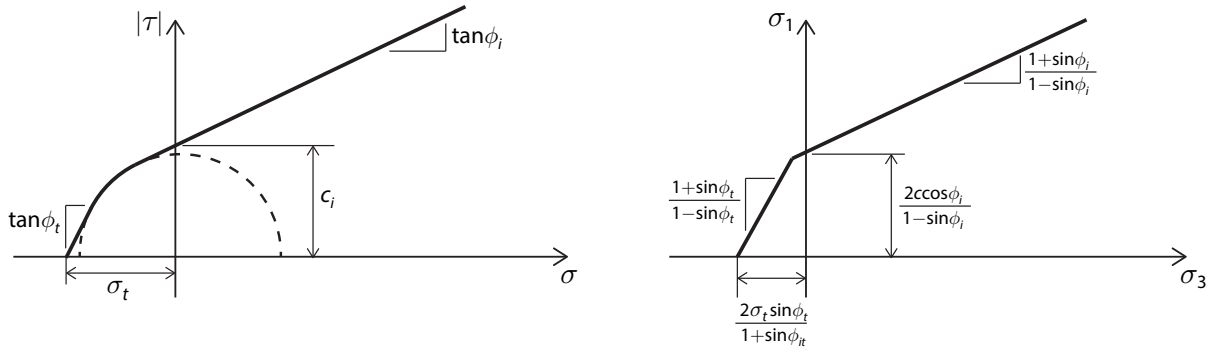

Fig. 4. Generalized Type B interface in σ-τ space (left) and in σ_1-σ_3 space (right).

3 Example

In the following, the differences between the two types of interface models are illustrated by the bearing capacity of a strip footing subjected to inclined and eccentric loading as shown in Figure 5. The numerical analyses are carried out using the finite element software OPTUM G2 which allows for the modelling of both types of interfaces.

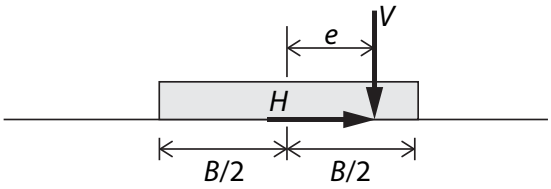

Fig. 5. Strip footing subjected to general loading.

For $e/B = 0$, Green (1954) has provided the following exact solution:

$$\frac{V}{Bs_u} = \begin{cases} \frac{1}{2}(2+\pi) + \arccos\left(\frac{H}{Bs_u}\right) + \sqrt{1-\left(\frac{H}{Bs_u}\right)^2} & \text{for } 0 \le \frac{H}{V} \le \frac{2}{(2+\pi)} \\ \frac{V}{H} & \text{otherwise} \end{cases} \tag{8}$$

Upper and lower bound limit analyses with the Type A interface are in excellent agreement with this solution (see Figure 6).

We now turn our attention to the Type B interface model. We would here expect the presence of the interface to have an influence for values of H/V in excess of 1. Setting $\sigma = V/B$ and $\tau = H/B$, the equation for the analogue to the limiting Mohr's circle shown in Figure 2 is given by

$$\left(\frac{V}{Bs_u} - 1\right)^2 + \left(\frac{H}{Bs_u}\right)^2 = 1 \tag{9}$$

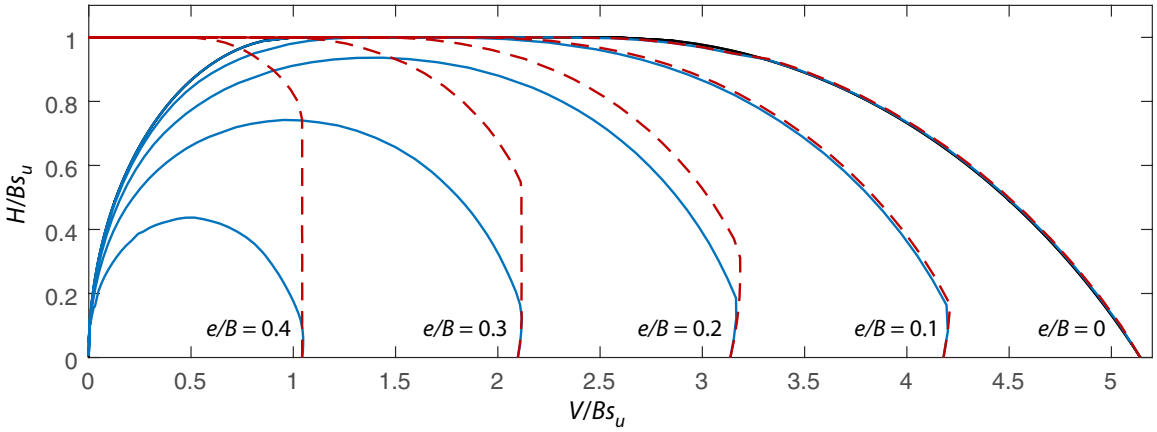

Fig. 6. V-H diagram for various eccentricities. Red dashed and blue full lines represent the results of the Type A and B interface models respectively. The Green solutions (original and modified) are shown by black full lines (hardly visible).

This leads to the following modification of Green's solution:

$$\frac{V}{Bs_u} = \begin{cases} \frac{1}{2}(2+\pi) + \arccos\left(\frac{H}{Bs_u}\right) + \sqrt{1-\left(\frac{H}{Bs_u}\right)^2} & \text{for } 0 \le \frac{H}{V} \le \frac{2}{(2+\pi)} \\ \frac{V}{H} & \text{for } \frac{2}{(2+\pi)} < \frac{H}{V} \le 1 \\ 1 - \sqrt{1-\left(\frac{H}{Bs_u}\right)^2} & \text{otherwise} \end{cases} \tag{10}$$

This is shown in Figure 6 along with numerical results using the Type B interface. Also shown are numerical results for different values of e/B. Comparing the results from the Type A and B interfaces, we see a relatively pronounced effect that increases as the eccentricity and/or angle of load inclination increases.

3.1 Other analytical estimates

It is interesting to note that the differences manifested by the two interface models are reflected in common analytical estimates. DNVGL-RP-C212 (DNV, 2017) suggests a solution given by

$$V = \tfrac{1}{2}(2+\pi)\left(1 + \sqrt{1 - \frac{\max(0, H - 2es_u)}{(B-2e)s_u}}\right)(B-2e)\,s_u, \quad H \le Bs_u \tag{11}$$

This solution, which is a modification of a solution due to Brinch Hansen (1970), is reminiscent of that resulting from the Type A interface in that it implies a maximum horizontal load of Bs_u for vertical loads less than or equal to $\frac{1}{2}(2+\pi)(B-2e)s_u$ (see Figure 7). The $H - 2es_u$ term in the above equation expresses that the 'effective' horizonal load is that acting along the effective width of the foundation. In other words, it is implicitly assumed that the remaining load acts along the part of the foundation not in contact with the soil

and hence has no effect in destabilizing it. This is consistent with the feature of the Type A model of being able to sustain the full shear capacity even for zero normal stress.

The bearing capacity theory of Meyerhof (1963), on the other hand, implies a maximum horizontal load given by

$$H = \min\left\{Bs_u, V\cot\left(\frac{\pi}{2}\sqrt{\frac{V}{(2+\pi)(B-2e)s_u}}\right)\right\}, \quad V \leq (2+\pi)(B-2e)s_u \tag{12}$$

The V-H diagrams are here qualitatively similar to those resulting from the Type B interface model. In particular, the feature that the curves pass through $(V, H) = (0, 0)$ is reproduced (see Figure 8). Meyerhof compared his expression to experimental data and good agreement was found, including for large eccentricities and angles of load inclination (Meyerhof, 1953). Compared to the Type B results, we see that the solution is mostly conservative.

Finally, EN 1997-1 (EC7, 2004) operates with the original Brinch Hansen (1970) expression which may be viewed as a compromise between the above solutions:

$$V = \tfrac{1}{2}(2+\pi)\left(1+\sqrt{1-\frac{H}{(B-2e)s_u}}\right)(B-2e), \quad H \leq (B-2e)s_u \tag{13}$$

The maximum horizontal force here scales with the effective width of the foundation though it remains finite for $V = 0$ (see Figure 9). This solution is reminiscent of the one proposed by Houlsby & Puzrin (1999). Compared to the Type B results, it is conservative up to relatively large load inclination angles (45° for $e/B = 0$ and more so for finite eccentricities).

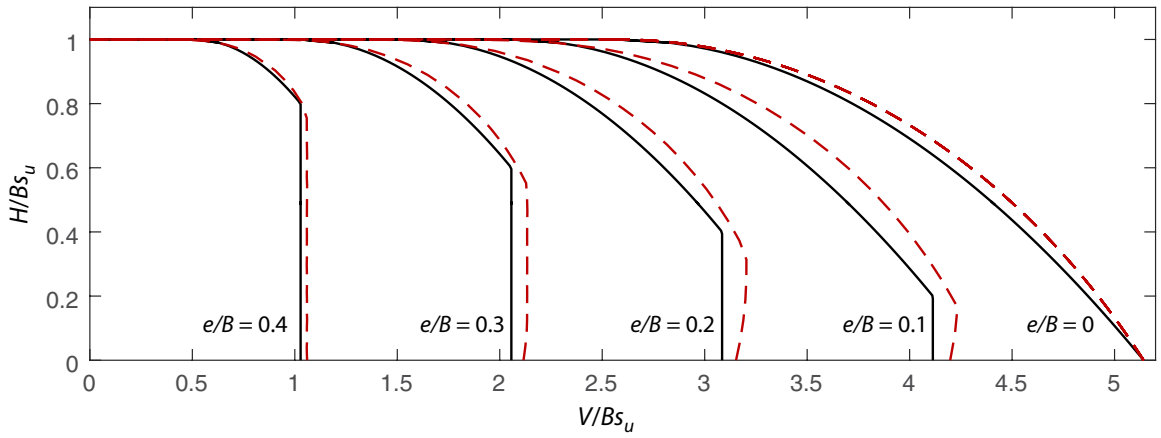

Fig. 7. V-H diagrams of DNV, 2017 (full) compared to results of Type A interface (dashed).

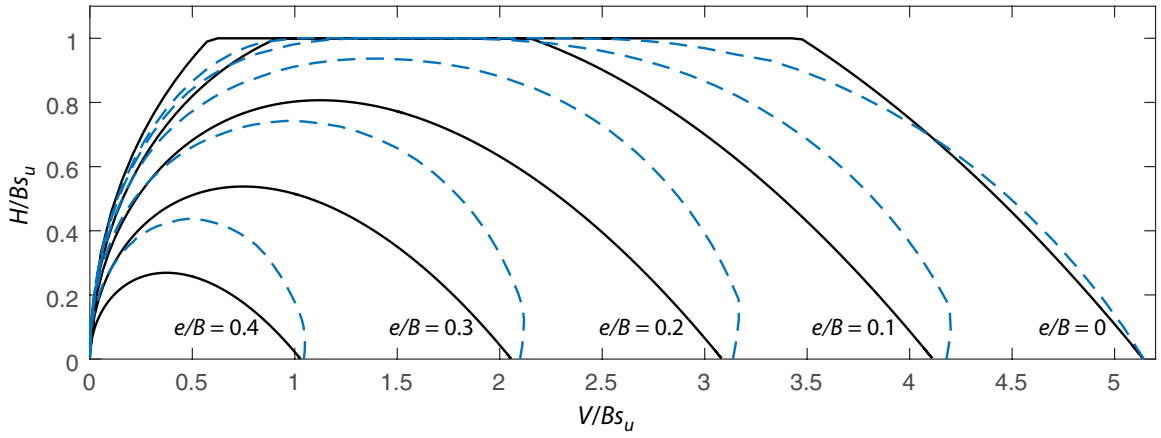

Fig. 8. V-H diagrams of Meyerhof, 1963 (full) compared to results of Type B interface (dashed).

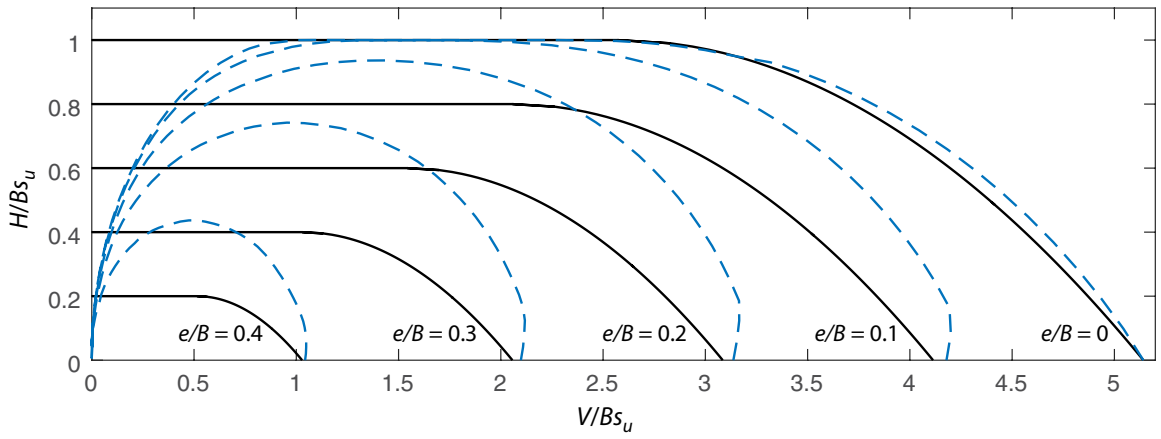

Fig. 9. V-H diagrams of EC7, 2004 (full) compared to results of Type B interface (dashed).

4 Conclusions

The differences between two common approaches to the modelling of interfaces have been discussed. The consequences of these differences have been demonstrated by the solution of a boundary value problem involving the undrained bearing capacity of a strip footing subjected to general loading. Though similar, the two interface models may under certain circumstances lead to fundamentally different results. While both models are reasonable in the sense that they prevent tensile normal stresses at interfaces, the Type B model additionally ensures that all principal stresses at the interface are compressive. As such, if the aim is to represent the interface as a thin layer of material incapable sustaining tension, the latter model is preferable.

References

Brinch Hansen, J. (1970). A revised and extended formula for bearing capacity, *DGI Bull.*, 28(17), 5–11.

DNV (2017). DNVGL-RP-C212: Offshore soil mechanics and geotechnical engineering, *DNV GL AS.*

EC7 (2004). EN 1997-1: 2004. Eurocode 7: Geotechnical design. Part 1: General rules, *CEN.*

Green, A. P. (1954). The plastic yielding of metal junctions due to combined shear and pressure, *J. Mech. Phys. Solids*, 2, 197–211.

Houlsby, G. T. & Puzrin, A. M. (1999). The bearing capacity of a strip footing on clay under combined loading, *Proc. R. Soc. Lond.*, 455, 893–916.

Meyerhof, G. G. (1953). The bearing capacity of foundations under eccentric and inclined loads, *Proc. 3rd Int. Conf. Soil Mechanics and Foundation Engineering, Zurich*, 1, 440–445.

Meyerhof, G. G. (1963). Some recent research on the bearing capacity of foundations, *Can. Geotech. J.*, 1(1), 16–26.

Wriggers, P. (2006). Computational Contact Mechanics, *Springer Verlag.*